

Single-Molecule Force Spectroscopy of Isolated and Aggregated Fibronectin Proteins on Negatively Charged Surfaces in Aqueous Liquids

Pamela Y. Meadows,[†] Jason E. Bemis,[‡] and Gilbert C. Walker^{*,†}

Department of Chemistry, University of Pittsburgh, Pittsburgh, Pennsylvania 15260, and
Asylum Research, Santa Barbara, California, 93117-5550

Received July 7, 2003. In Final Form: September 25, 2003

Plasma fibronectin (FN) was adsorbed to negatively charged surfaces, and the mechanical behavior of both isolated and aggregated FN molecules was observed using molecular force spectroscopy. Images of FN molecules show that the isolated proteins are already partially denatured, and mechanically pulling on them yields force transitions at distance intervals significantly shorter than the domains' contour lengths. Only when FN was aggregated on the surface did force transitions occur at length intervals corresponding to Type III domain lengths. Apparently, FN's density on the surface plays a critical role in protein stabilization. The dependence of the transition forces on the loading rates was also measured and modeled. In measurements done on single proteins in aggregates, one barrier in the direction of the applied force was observed, which arose from domain denaturation; however, studies of isolated, single molecules revealed two barriers, where both arise from protein-surface interactions.

Introduction

When a surface is exposed to an aqueous solution of protein, it typically becomes covered by a proteinaceous film. For cardiovascular implants, protein deposition can then lead to adverse responses within the host. These include, but are not limited to, cellular adhesion, activation, and formation of thrombi, which can then detach forming possibly life-threatening emboli.^{1,2} To eliminate or minimize thrombogenesis on implant materials and other protein deposition effects, many groups have begun to explore the mechanism behind protein adsorption.³⁻⁸ Changes in the state of hydration of both the substrate and the protein as well as rearrangement of the protein's structure and redistribution of its charged groups are a few of the factors involved in protein adsorption.³⁻⁸ In addition to these intermolecular forces, surface chemistry,⁹⁻¹⁵ topography,¹⁵⁻¹⁷ protein concentration, solvent

viscosity, and ionic strength¹⁸ have also been found to play critical roles in regulating protein and cellular adhesion. In the work presented here, we examine the mechanical behavior of an adhesion-promoting protein physisorbed to negatively charged surfaces using an atomic force microscope (AFM).

Atomic force microscopy has become a widely used tool for measuring inter- and intramolecular interactions; ligand-receptor adhesion forces,¹⁹ polymer elasticity²⁰⁻²⁴ and conductivity,²⁵ DNA²⁶ and RNA²⁷ folding kinetics, and the elastic properties of proteins in the extracellular matrix²⁸⁻³² have been studied. Here, we use an AFM as a single-molecule force probe to study the mechanical properties of fibronectin (FN) at negatively charged surfaces. The basic methodology behind an AFM and the interpretation of the data collected will not be discussed here because of the extensive work already reported in the literature.³³⁻³⁹

* Author to whom correspondence should be addressed. E-mail: gilbertw@pitt.edu.

[†] University of Pittsburgh.

[‡] Asylum Research.

(1) Haycox, C. L.; Ratner, B. D. *J. Biomed. Mater. Res.* **1993**, *27*, 1181.

(2) Bruck, S. D. *Biomater., Med. Devices, Artif. Organs* **1983-84**, *11*, 271.

(3) Hlady, V.; Buijs, J. *Curr. Opin. Biotechnol.* **1996**, *7*, 72.

(4) Norde, W.; Favier, J. P. *Colloids Surf.* **1992**, *64*, 87.

(5) Brash, J. L.; Horbett, T. A., Eds.; *Proteins at Interfaces II: Fundamentals and Applications*; American Chemical Society: Washington, DC, 1995.

(6) Haynes, C. A.; Norde, W. *Colloids Surf., B* **1994**, *2*, 517.

(7) Norde, W. *Adv. Colloid Interface Sci.* **1986**, *25*, 267.

(8) Haynes, C. A.; Norde, W. *J. Colloid Interface Sci.* **1995**, *169*, 313.

(9) Lestelius, M.; Liedberg, B.; Tengvall, P. *Langmuir* **1997**, *13*, 5900.

(10) Scotchford, C. A.; Gilmore, C. P.; Cooper, E.; Leggett, G. J.; Downes, S. *J. Biomed. Mater. Res.* **2002**, *59*, 84.

(11) Sigal, G. B.; Mrksich, M.; Whitesides, G. M. *J. Am. Chem. Soc.* **1998**, *120*, 3464.

(12) Mrksich, M. *Cell. Mol. Life Sci.* **1998**, *54*, 653.

(13) Grinnell, F.; Feld, M. K. *J. Biomed. Mater. Res.* **1981**, *15*, 363.

(14) Kidoaki, S.; Matsuda, T. *Langmuir* **1999**, *15*, 7639.

(15) Denis, F. A.; Hanarp, P.; Sutherland, D. S.; Gold, J.; Mustin, C.; Rouxhet, P. G.; Duffrene, Y. F. *Langmuir* **2002**, *18*, 819.

(16) McFarland, C. D.; Thomas, C. H.; DeFilippis, C.; Steele, J. G.; Healy, K. E. *J. Biomed. Mater. Res.* **2000**, *49*, 200.

(17) Duffrene, Y. F.; Marchal, T. G.; Rouxhet, P. G. *Langmuir* **1999**, *15*, 2871.

(18) Tripp, B. C.; Magda, J. J.; Andrade, J. D. *J. Colloid Interface Sci.* **1995**, *173*, 16.

(19) Florin, E.; Moy, V. T.; Gaub, H. E. *Science* **1994**, *264*, 415.

(20) Bemis, J.; Akhremitchev, B.; Walker, G. *Langmuir* **1999**, *15*, 2799.

(21) Smith, B. L.; Schaeffer, T. E.; Viani, M.; Thompson, J. B.; Frederick, N. A.; Kindt, J.; Belcher, A.; Stucky, G. D.; Morse, D. E.; Hansma, P. K. *Nature* **1999**, *399*, 761.

(22) Zhang, W. K.; Zou, S.; Wang, C.; Zhang, X. J. *J. Phys. Chem. B* **2000**, *104*, 10258.

(23) Al-Maawali, S.; Bemis, J. E.; Akhremitchev, B. B.; Lecharoen, R.; Janesko, B. G.; Walker, G. C. *J. Phys. Chem. B* **2001**, *105*, 3965.

(24) Ortiz, C.; Hadziioannou, G. *Macromolecules* **1999**, *32*, 780.

(25) Tivanski, A. V.; Bemis, J. E.; Akhremitchev, B. B.; Liu, H.; Walker, G. C. *Langmuir* **2003**, *19*, 1929.

(26) Strunz, T.; Oroszlan, K.; Schafer, R.; Guntherodt, H. *Proc. Natl. Acad. Sci. U.S.A.* **1999**, *96*, 11277.

(27) Liphardt, J.; Onoa, B.; Smith, S. B.; Tinoco, I., Jr.; Bustamante, C. *Science* **2001**, *292*, 733.

(28) Kellermayer, M. S. Z.; Smith, S. B.; Bustamante, C.; Granzier, H. L. *Biophys. J.* **2001**, *80*, 852.

(29) Tskhovrebova, L.; Trinick, J.; Sleep, J. A.; Simmons, R. M. *Nature* **1997**, *387*, 308.

(30) Rief, M.; Gautel, M.; Oesterheld, F.; Fernandez, J. M.; Gaub, H. E. *Science* **1997**, *276*, 1109.

(31) Oberhauser, A. F.; Marszalek, P. E.; Erickson, H. P.; Fernandez, J. M. *Nature* **1998**, *393*, 181.

(32) Law, R.; Carl, P.; Harper, S.; Dalhaimer, S.; Speicher, D. W.; Discher, D. E. *Biophys. J.* **2003**, *84*, 533.

(33) Zlatanova, J.; Lindsay, S. M.; Leuba, S. H. *Prog. Biophys. Mol. Bio.* **2000**, *74*, 37.

FN was chosen as the focus of this study because of its ability to bind numerous molecules such as heparin, fibrin, and collagen, but in particular, because of its role in mediating cellular adhesion to surfaces within the bloodstream and the extracellular matrix.^{40,41} FN is a 450 kDa glycoprotein that is composed of nearly two identical polypeptide chains linked near their carboxyl termini via two disulfide bonds. Each monomer is composed of 12 Type I, 2 Type II, and 17 Type III domains.^{40,41} Both the Type I and the Type II domains possess disulfide bonds whose strength precludes their mechanical denaturation in the force-extension experiments reported here; however, Type III domains, which lack disulfide bonds, can be mechanically denatured, and it is also these domains that are responsible for cellular binding.

We found that the density of protein adsorption plays a significant role in enabling domain denaturation by force spectroscopy. In the experiment, the protein was adsorbed to a surface; the tip was brought into contact with the protein and pulled away from the substrate, extending the protein between the tip and the surface. When FN was isolated on the surface, the transitions observed in the force versus distance data occurred at lengths and with forces uncharacteristic of Type III domain unfolding events, suggesting the proteins were already pre-denatured on the surface. Only when the proteins were aggregated on the surface were force transitions observed at distance intervals characteristic of domain denaturation. Apparently, FN is stabilized by the presence of neighboring molecules, which prevents its surface denaturation. A loading-rate analysis confirmed this as well. These plots suggest that the short lengths and small rupture forces observed were most likely due to a specific surface-protein interaction.

Experimental Details

General Procedures. All glassware and glass substrates (Ted Pella, Inc., Redding, CA) were soaked overnight in a base bath containing 500 g of KOH (J. T. Baker Scientific Equipment Company, Aston, PA), 500 mL of tap water, and 4 L of isopropanol (VWR International, Inc., Bridgeport, NJ). Water used in these experiments was purified to 18 M Ω -cm resistivity using a Barnstead NANO pure filter.

Solution Preparation. Bovine fibronectin from plasma (Sigma, St. Louis, MO) was used to prepare a 20 μ g/mL solution in phosphate buffered saline [PBS; 10 mM Na₂HPO₄ (J. T. Baker), 138 mM NaCl (Sigma), and 2.7 mM KCl (Mallinckrodt, Phillipsburg, NJ)] with 1% NaN₃ (Sigma). The solution was stored at 4 °C. The 1 M and 4 M guanidinium hydrochloride (GdmHCl) solutions (Sigma) were also prepared for experiments involving protein denaturation by added salt.

Sample Preparation. Mica (SPI, West Chester, PA) was attached via epoxy to a glass microscope slide (VMR Scientific, Inc., West Chester, PA). A total of 45 μ L of 1 μ g/mL FN solution was deposited on a freshly cleaved mica surface for 5 min, followed by gentle rinsing of the surface with 3 mL of water. The surface was then dried using a strong flow of nitrogen before imaging in neat water, PBS, or GdmHCl solutions. Experiments involving

protein denaturation followed a similar procedure, except the protein was denatured before being exposed to the surface, and the denaturant was also used as the imaging solvent. To prepare aggregated protein samples, the surfaces were allowed to remain under a 20 μ g/mL FN solution at 4 °C for 18–24 h before imaging in H₂O or PBS.

AFM Cantilevers. Olympus gold-coated cantilevers were purchased from Asylum Research (Santa Barbara, CA) and used as received from the company. Contact Si₃N₄ cantilevers from Digital Instruments–Veeco Metrology (Santa Barbara, CA) were allowed to soak for 1.5 h in a 1:10 (v/v) solution of diluted HF/H₂O.⁴² The spring constants ranged from 30 to 70 pN/nm and were determined using the thermal noise method.

AFM Measurements/Analysis. All measurements were obtained using molecular force probes from Asylum Research, which were capable of moving a cantilever in one dimension (MFP-1D) or in three dimensions for surface imaging (MFP-3D). The instruments were controlled with Igor Pro 4.01 (MFP-1D) or 4.05A (MFP-3D; Wavemetrics, Lake Oswego, OR) with a modified version of the MFP software 1.30R1 (MFP-1D) or 0.9r1 (MFP-3D). For the MFP-3D measurements, the tip was brought within 10 μ m of the surface, and the system was allowed to thermally equilibrate for at least 2 h before data collection. Images were obtained in an intermittent contact mode using a gold-coated cantilever with a tip oscillation of 60–70 nm. All force-extension curves were collected at a piezo *z* velocity of 1 μ m/s. Data analysis was performed using software written in Matlab (Math Works, Inc., Natick, MA).

Results and Discussion

Mechanical Behavior of Single Molecules of FN on a Mica Substrate. Images of the prepared samples were collected followed by molecular pulling experiments in region-specific surface areas. Figure 1 shows two images collected underwater, one of a control surface and one of FN deposited for 5 min. As can be seen, FN adopts a compact conformation in this solvent. Lin et al.⁴³ have observed FN in a more extended conformation when adsorbed to mica but in the absence of a solvent. Under these same conditions, we too have observed a less compact structure; however, in water, FN became more compact, appearing to redistribute its charged groups. PBS, although resembling physiological conditions, could not be used in these studies because protein desorption prevailed. Tip contamination under these buffered conditions was often observed as well.

Before conducting the molecular pulling experiments, it was necessary to confirm that the larger objects seen in Figure 1 were indeed single FN molecules rather than aggregates because smaller objects were also observed on the substrate. In a rough approximation, the minimum height required for a single FN molecule to adopt a spherical conformation was calculated to be 10 nm. This estimate indicates that the larger objects seen in Figure 1 are not aggregates but single molecules of FN, which were then chosen for the pulling experiments. Thus, immersion of the substrate in a protein solution with a concentration of 1 μ g/mL for 5 min was sufficient to obtain numerous but isolated protein molecules on the surface.

A number of steps were taken to ensure that single-molecule experiments were accomplished using only uncontaminated tips. First, images were collected in an intermittent contact mode followed by force-extension plots on *selected* regions of the surface, which provides a great advantage over random sampling of the surface area. Selecting the molecule to pull helps to ensure that only isolated, single molecules on the surface are probed. The

(34) Hugel, T.; Seitz, M. *Macromol. Rapid Commun.* **2001**, *22*, 989.

(35) Fisher, T. E.; Marszalek, P. E.; Oberhauser, A. F.; Carrion-Vazquez, M.; Fernandez, J. M. *J. Physiol.* **1999**, *520*, 1, 5.

(36) Ludwig, M.; Rief, M.; Schmidt, L.; Li, H.; Oesterhelt, F.; Gautel, M.; Gaub, H. E. *Appl. Phys. A* **1999**, *68*, 173.

(37) Willemsen, O. H.; Snel, M. M. E.; Cambi, A.; Greve, J.; De Grooth, B. G.; Figdor, C. G. *Biophys. J.* **2000**, *79*, 3267.

(38) Fisher, T. E.; Oberhauser, A. F.; Carrion-Vazquez, M.; Marszalek, P. E.; Fernandez, J. M. *Trends Biochem. Sci.* **1999**, *24*, 379.

(39) Makarov, D. E.; Wang, Z.; Thompson, J. B.; Hansma, H. G. *J. Chem. Phys.* **2002**, *116* (17), 7760.

(40) McDonagh, J., Ed.; *Plasma Fibronectin, Structure and Function*; Marcel Dekker: New York, 1985.

(41) Mosher, D., Ed.; *Biology of Extracellular Matrix: A Series Fibronectin*; Academic Press: San Diego, 1989.

(42) Caution! HF is a highly toxic solution and is extremely dangerous to work with; chemical-resistant gloves, goggles, and an 8-in. minimum diameter face shield should be worn.

(43) Lin, H.; Lal, R.; Clegg, D. O. *Biochemistry* **2000**, *39*, 3192.

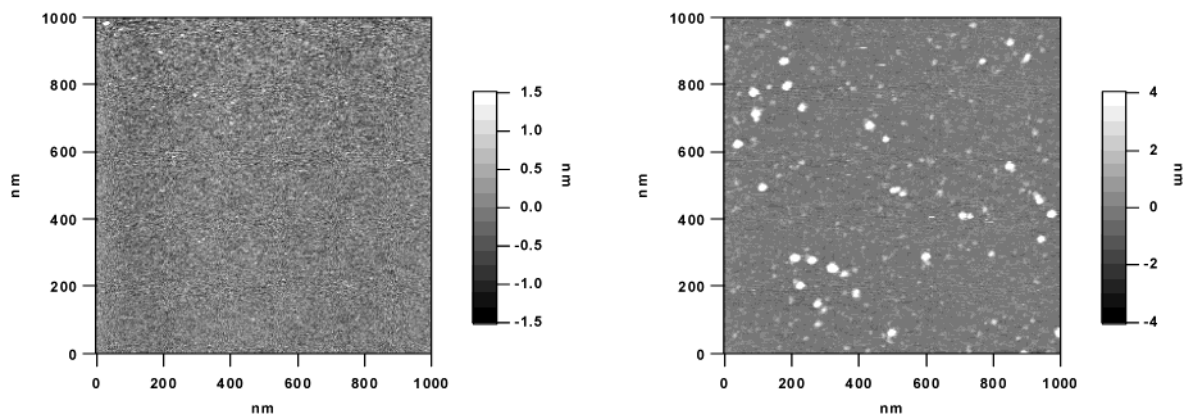


Figure 1. Two images showing before (left) and after (right) sparse protein deposition on mica. The larger molecules in the right image are single molecules of FN. The smaller objects are probably protein fragments. As can be seen in the height scale, the isolated proteins are greater than 8 nm in height.

Table 1. Summary of a Typical Force Spectroscopy Experiment on Single Molecules Collected in Water on a Mica Substrate

breakdown of force plots collected	number
force plots collected	12 133
force plots where FN is contacted	10 853
force plots where FN is contacted and adsorbs	1 908
single rupture force plots	877
multiple rupture force plots used for analysis	853 ^a
total number of ruptures used in these plots	2 679

^a Force plots with rupture forces near the limit of our resolution were excluded.

177 proteins were also imaged on the surface before and after
 178 pulling, indicating that the proteins remained on the
 179 substrate. Further confirmation that the tip had not
 180 become contaminated was obtained by collecting force plots
 181 on bare regions of the substrate after protein probing.
 182 Less than 0.1% of the force plots showed stretching events,
 183 which makes it unlikely that the tip in previous force
 184 plots had been fouled with protein. High-resolution
 185 topographic imaging was also done after the pulling
 186 experiments; these images cannot be obtained if the tip
 187 has become fouled with protein. Thus, the combination of
 188 imaging with spatially specific pulling measurements
 189 gives great confidence that the data obtained is due to the
 190 mechanical stretching of a single, isolated FN molecule
 191 that remained adhered to the substrate.

192 Table 1 summarizes the data collected in one of the
 193 imaging and protein pulling experiments. The surface-
 194 bound protein physisorbed to the tip in approximately
 195 18% of the force plots, and in almost half of these
 196 occurrences, only one force transition resulted, indicative
 197 of protein–tip rupture. The remaining force–distance
 198 curves, which show multiple ruptures, were analyzed for
 199 their relation to protein dynamics. Figure 2 displays a
 200 force plot containing two relevant force transitions as well
 201 as a plot of the difference in length (ΔL) between successive
 202 ruptures. This length was calculated using the points of
 203 the cantilever's maximum extension. A most probable
 204 length of 9.2 ± 0.4 nm was observed when all transition
 205 lengths were included in the fitted distribution, and a
 206 most probable length of 9.5 ± 0.5 nm was observed when
 207 the last transition length (gap between the second to last
 208 and last rupture) was excluded in the distribution (as
 209 shown in Figure 2). These lengths do not correlate with
 210 the values reported in the literature (25.1 ± 0.5^{44} or 28.5
 211 ± 4.0 nm)⁴⁵ for Type III domain denaturation events in

212 the protein tenascin45 or for 0.2 mg/mL FN adsorbed on
 213 a Petri dish.⁴⁴ However, Oberhauser et al.⁴⁶ did observe
 214 a peak at 9.3 ± 1.6 nm when pulling a polypeptide
 215 containing the first Type III domain. Although this
 216 represented the minority of their data, this length clearly
 217 dominates the results reported here, as seen in Figure 2.

218 Possible explanations for this short length could be the
 219 result of interdomain interactions, domain intermediates,
 220 or a specific surface–protein interaction. To examine the
 221 potential role of interdomain interactions, a 1 M GdmHCl
 222 solution was used to minimize these forces.⁴⁷ In these
 223 denaturing solutions, more extended protein conforma-
 224 tions were observed in the surface images (data not shown),
 225 confirming these interactions had been reduced; however,
 226 the most probable length interval obtained was ~ 14 nm
 227 (Supporting Information, Figure S1). This slightly longer
 228 length interval is consistent with the denaturant partly
 229 extending the protein on the surface, but it is still shorter
 230 than what would be expected for entire domain unfolding.

231 An unfolding intermediate could also generate the 9.5-
 232 nm length interval. Several steered molecular dynamics
 233 simulations have been performed on FN; Gao et al.⁴⁸ have
 234 shown an intermediate at 10 nm, which occurs when the
 235 A and B strands of the 10th Type III domain unravel prior
 236 to the interstrand hydrogen bonds breaking between the
 237 F and G strands. Oberhauser et al.⁴⁶ assigned this
 238 phenomenon to the 9.3-nm transition length they observed
 239 in the polypeptide containing the first Type III domain.
 240 To determine if the short length observed in this work
 241 was indeed a result of an intermediate, FN was denatured
 242 using 4 M GdmHCl, a concentration documented to
 243 denature the entire protein in solution.⁴⁷ Unfortunately,
 244 with this high concentration, salt deposition prevented
 245 successful pulling experiments. Thus, an intermediate
 246 contributing to the 9.5-nm length interval has not been
 247 excluded, but as will be discussed next, force plots
 248 illustrating this length interval indicate the forced separa-
 249 tion of the protein from the surface.

250 **Mechanical Behavior of FN Aggregates.** Because
 251 extending isolated single molecules of FN did not produce
 252 force transitions at length intervals previously associated
 253 with Type III domain unfolding events, we explored the
 254 possibility that the protein had undergone partial surface

(45) Oberhauser, A. F.; Marszalek, P. E.; Erickson, H. P.; Fernandez, J. M. *Nature* **1998**, *393*, 181.

(46) Oberhauser, A. F.; Badilla-Fernandez, C.; Carrion-Vazquez, M.; Fernandez, J. M. *J. Mol. Biol.* **2002**, *319*, 433.

(47) Khan, M. Y.; Medow, M. S.; Newman, S. A. *Biochem. J.* **1990**, *270*, 33.

(48) Gao, M.; Craig, D.; Vogel, V.; Schulten, K. *J. Mol. Biol.* **2002**, *323*, 939.

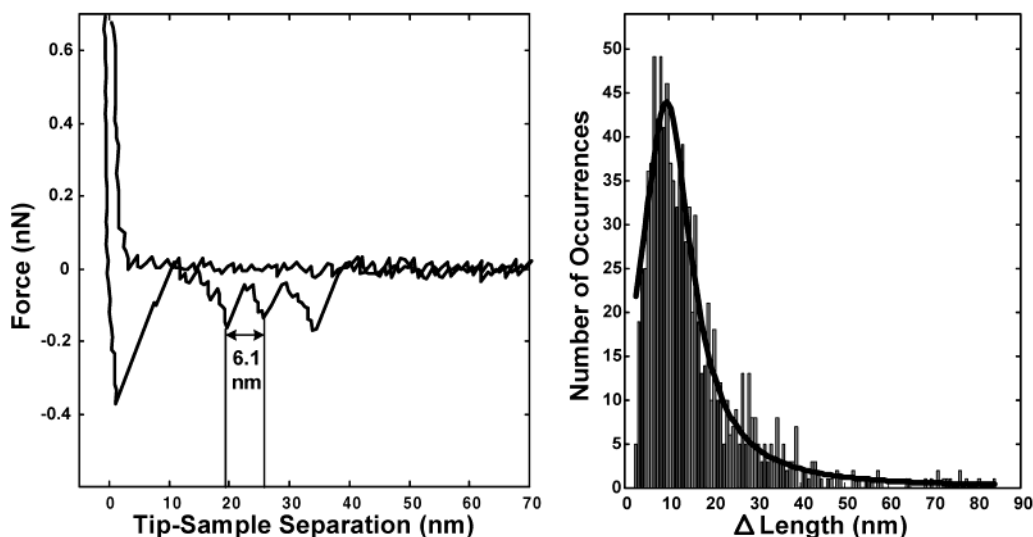


Figure 2. Force plot obtained when extending single molecules of FN away from a mica surface in water (left panel). The length intervals between successive ruptures was determined by subtracting the difference in tip–sample separations at points prior to the cantilever returning to near zero force, as illustrated by the vertical lines. The right panel gives a histogram of these length intervals; the most probable value of 9.5 ± 0.5 nm was determined by a Lorentzian fit to the data.

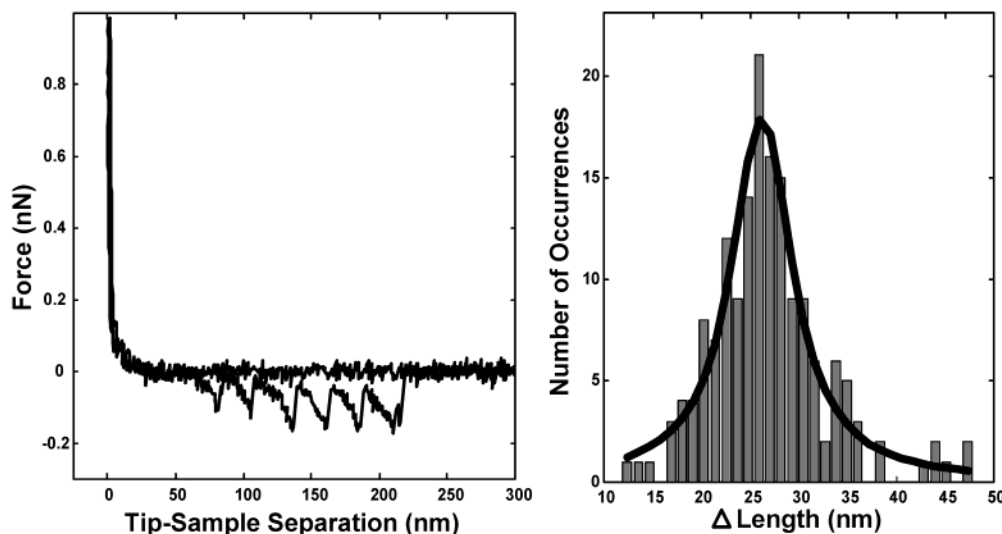


Figure 3. Force plot obtained when extending molecules in aggregates of FN from mica (left panel). A histogram of the difference in length between successive ruptures is seen on the right. The Lorentzian fit of the data shows a length of approximately 26.2 ± 0.6 nm. This length is similar to the length interval reported in the literature,^{44,45} where it was ascribed to the unfolding of a Type III domain. It is important to point out that, when the protein is aggregated, the force plots often show complex intermolecular interactions in addition to these equally spaced microruptures.

255 denaturation. Several groups^{4–5,13,49} have observed that
 256 low-density protein coverage results in a conformationally
 257 inactive protein and only at a higher coverage does the
 258 protein become stable. Neighboring proteins, thus, prevent
 259 domain denaturation¹³ at the surface, perhaps by protect-
 260 ing the domains from interacting with the surface. Figure
 261 3 reveals a force plot obtained for samples of densely
 262 deposited FN as well as a histogram of ΔL for these regular,
 263 repeating microruptures. The peak shifts from 9.5 ± 0.5
 264 to 26.2 ± 0.6 nm, a length interval agreeing quite well
 265 with literature reports for domain unfolding events. When
 266 varying environmental factors such as the solvent,
 267 substrate, and tip material, negligible differences in the
 268 length were observed for densely covered surfaces; the
 269 domain unfolding events were always present but the
 270 rupture forces did vary. Table 2 summarizes the results

Table 2. Summary of the Rupture Forces and Differences in Length between Successive Ruptures

experimental conditions	Δ length (nm) ^a	rupture force (pN)
mica/Au tip/water/ isolated single molecules	9.2 ± 0.4	113.5 ± 2.6
mica/Au tip/1 M GdmHCl/ isolated single molecules	14.5 ± 1.3	80.8 ± 2.9
mica/Au tip/water/dense FN coverage	26.2 ± 0.6	170.2 ± 4.2
mica/Au tip/PBS/dense FN coverage	27.1 ± 0.3	166.3 ± 2.5
glass/Au tip/water/dense FN coverage	26.2 ± 0.6	204.0 ± 3.2
glass/Au tip/PBS/dense FN coverage	26.8 ± 0.4	154.1 ± 1.9
glass/Si ₃ N ₄ /PBS/dense FN coverage	25.7 ± 0.3	125.4 ± 1.1

^a Values from the Δ length distributions include the last rupture within a force plot, unlike the values reported here for the force distribution plots.

for all experiments conducted, while Supporting Information Figures S1–3 show the distributions of the data obtained. In general, higher rupture forces were obtained with a gold-coated tip than with a silicon nitride cantilever, 271
 272
 273
 274

(49) Steadman, B. L.; Thompson, K. C.; Middaugh, C. R.; Matsuno, K.; Vrona, S.; Lawson, E. Q.; Lewis, R. V. *Biotechnol. Bioeng.* **1992**, *40*, 8.

275 and as expected, the rupture forces in a denaturant were
 276 smaller. Furthermore, the rupture transition forces in the
 277 single-molecule studies were smaller than those observed
 278 in the aggregate studies that probed the domain unfolding
 279 events.

280 **Transition State Crossing under an Applied Force.**

281 To gain insight into the energy landscape traversed during
 282 the forced extension of proteins, the relationship between
 283 the transition (rupture) force and the rate at which the
 284 force was applied to the system was explored. On the basis
 285 of the work from Bell and Evans et al.,^{50–56} an exponential
 286 relationship exists between the rate of dissociation (k_{off})
 287 of a ligand–receptor complex and the externally applied
 288 force F (eq 1).

$$k_{\text{off}}(F) = k_{\text{off}}(0)e^{F x_{\beta} / k_B T} \quad (1)$$

289 Here, $k_B T$ represents the thermal energy, $k_{\text{off}}(0)$ is the
 290 rate of dissociation under zero applied force, and x_{β} is the
 291 distance from the free energy minimum to the transition
 292 state from the ground state projected along the direction
 293 of the applied force. For the force applied in the x direction,
 294 the free energy for dissociation decreases linearly with
 295 the applied force (eq 2).

$$\Delta G^{\ddagger}(F) = \Delta G^{\ddagger}(0) - F x_{\beta} \quad (2)$$

296 As this force is applied to a system, the observed
 297 unbinding force will depend on the rate at which the force
 298 is applied to the system, that is, the loading rate. As eq
 299 3 illustrates, there is a logarithmic dependence of this
 300 dissociation force (F) on the loading rate (r).^{51–58}

$$F = \frac{k_B T}{x_{\beta}} \ln \left(\frac{x_{\beta} r}{k_{\text{off}}(0) k_B T} \right) \quad (3)$$

301 Over several orders of magnitude, a plot of the rupture
 302 force versus $\ln(r)$ will reveal linear regions of increasing
 303 slope, each region corresponding to a barrier traversed
 304 along the direction of the applied force. Using eq 3 then
 305 allows x_{β} to be determined, and extrapolating back to zero
 306 applied force, $k_{\text{off}}(0)$ and $\Delta G^{\ddagger}(0)$ can be determined through
 307 eqs 4 and 5, where h is Planck's constant.

$$k_{\text{off}}(0) = \frac{r x_{\beta}}{k_B T} \quad (4)$$

$$k_{\text{off}}(0) = \frac{k_B T}{h} e^{-\Delta G^{\ddagger} / k_B T} \quad (5)$$

308 Thus, from a loading-rate plot, the thermodynamic
 309 parameters involved in ligand–receptor dissociation via
 310 atomic force microscopy can be approximated.

311 However, as pointed out by Evans, unlike a ligand–
 312 receptor scenario, which displays linear elastic properties,
 313 the application of force on proteins or highly flexible

polymers results in nonlinear elastic stretches. The model
 described briefly above works well for the first example,
 yet complications can arise for the latter case,^{51,54} when
 determining the rupture force dependence on the loading
 rate. Nevertheless, Rief et al.³⁰ and Carrion-Vasquez et
 al.⁵⁹ have observed a linear dependence of the unbinding
 force versus the logarithm of the loading rate when
 mechanically unfolding proteins. Therefore, this model
 will be applied here to determine the thermodynamic
 parameters associated with forced unfolding.

In the data presented below, the rupture force was
 determined from the force plots using the data point just
 prior to where the cantilever returns to its rest position,
 that is, the point of maximum extension of the cantilever.
 The loading rate (r) was also determined directly from the
 force plots through eq 6

$$r_{\text{rupture}} = \Delta F \left(\frac{n+1}{S_{\text{rate}}} \right) \quad (6)$$

where n is 1 less than the number of points used to obtain
 ΔF , S_{rate} is the sampling rate in the data acquisition in
 points/s, and ΔF is the change in the attractive force from
 the point of rupture to five points previous to the rupture.

Figure 4 shows three loading-rate plots that were
 obtained while Table 3 gives the corresponding parameters
 using the mean values for the force and loading rates. In
 the analysis represented by panels A and B, the last
 rupture in the force plots was omitted to exclude the
 process of the protein breaking free from the tip. As can
 be seen in Figure 4B, the regular repeating ruptures
 observed in Figure 3 of the protein aggregate studies
 produced only one linear region in the loading-rate plot.
 However, the isolated single-molecule studies showed two
 linear regions. Analysis of the data gives an acceptable
 value for the barrier position for the shallow sloped region
 in Figure 4A but an unphysical barrier position (~ 0.02
 nm) for the steeper linear region of the data. Furthermore,
 in agreement with our previous conclusions, Table 3 also
 reveals that a higher surface density of proteins provides
 added kinetic stability.

It was suggested previously that either a substructure
 of a domain or a specific surface–protein interaction could
 give rise to the uncharacteristic force and ΔL values that
 were obtained. To test for a surface–protein interaction,
 the rupture forces from force plots displaying only one
 stretching event, indicative of protein–tip rupture, were
 plotted as a function of the loading rate (Figure 4C). As
 can be seen in this panel, two linear regions were found
 with the distances to the barriers being similar to those
 found in the single-molecule studies. Therefore, because
 the last rupture had been removed from the analysis in
 panels A and B of Figure 4 and panel C reveals a specific
 surface–protein interaction involving two barriers, we
 conclude that a protein–surface interaction is indeed
 occurring in the isolated, single-molecule studies and is
 apparently the dominant state.

Because the second linear region seen in Figure 4A could
 be fit by the model but the distance to the barrier is
 unphysical, an alternative model is needed. A more
 realistic barrier position (a few bond lengths) might be
 obtained if it is assumed that the direction of the applied
 force is at a considerable angle to the initial direction for
 the surface dissociation, but the validity of this assumption
 and the other assumptions of eq 3 along with the role of

(50) Bell, G. I. *Science* **1978**, *200*, 618.

(51) Evans, E. *Annu. Rev. Biophys. Biomol. Struct.* **2001**, *30*, 105.

(52) Evans, E. *Faraday Discuss.* **1998**, *111*, 1.

(53) Evans, E.; Ludwig, F. J. *Phys.: Condens. Matter* **2000**, *12*, A315.

(54) Evans, E.; Ritchie, K. *Biophys. J.* **1999**, *76*, 2439.

(55) Merkel, R.; Nassoy, P.; Leung, A.; Ritchie, K.; Evans, E. *Nature* **1999**, *397*, 50.

(56) Evans, E.; Ritchie, K. *Biophys. J.* **1997**, *72*, 1541.

(57) Strunz, T.; Oroszlan, K.; Schumakovitch, I.; Guntherodt, H.-J.; Hegner, M. *Biophys. J.* **2000**, *79*, 1206.

(58) Dettmann, W.; Grandbois, M.; Andre, S.; Benoit, M.; Wehle, A. K.; Kaltner, H.; Gabius, H.; Gaub, H. E. *Arch. Biochem. Biophys.* **2000**, *383*, 157.

(59) Carrion-Vasquez, M.; Oberhauser, A. F.; Fowler, S. B.; Marszalek, P. E.; Broedel, S. E. B.; Clarke, J.; Fernandez, J. M. *Proc. Natl. Acad. Sci. U.S.A.* **1999**, *96*, 3694.

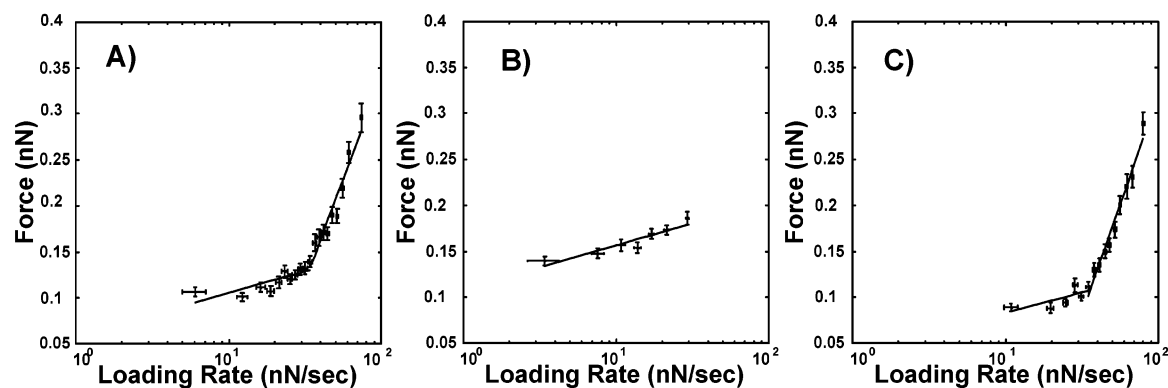


Figure 4. Plots illustrating the relationship between the rupture force and loading rate. The binned points represent the mean values of the force and loading rate while the error bars correspond to the standard deviation of the mean. Plot A corresponds to measurements performed on single FN molecules isolated on a mica substrate in water. Plot B represents FN densely deposited on a glass substrate in PBS. In both of these plots, the last rupture in the force plots, which corresponds to the rupture of the protein from the tip, is excluded from the analysis. In plot C, rupture forces in plots with only one pulling event are analyzed for isolated single FN molecules on mica in water, which, therefore, includes the protein–tip rupture. Under the Bell model and its extensions, each linear region corresponds to a barrier crossing process in the forced extension of the protein between the tip and the substrate. The shallow sloped regions correspond to transitions between protein states that occur via rate processes that are plausible when modeled with a preexponential factor of $k_B T/h$. The sloped feature in panel B implies reaction coordinate parameters similar to those previously observed by Oberhauser et al.⁴⁶ The steeper, second linear regions in plots A and C yield a nonphysical barrier position; it is also probable that frictions along these barrier crossings are much greater than that observed in panel B. Such a larger friction is probably due to the damped dynamics of protein bound to the substrate in A and the tip in C.

Table 3. Unfolding Barrier Positions and Energies

experimental conditions	x_β (nm)	$\Delta G(0)$ (kcal/mol)
mica/Au tip/water/isolated single molecules	0.20 ± 0.05	16.8 ± 0.60
	$0.021 \pm 2.0 \times 10^{-3}$	14.7 ± 0.28
mica/Au tip/1 M GdmHCl/isolated single molecules	0.19 ± 0.06	16.4 ± 0.66
	$0.013 \pm 7.0 \times 10^{-4}$	15.0 ± 0.15
mica/Au tip/water/dense FN coverage	0.19 ± 0.07	18.2 ± 1.3
mica/Au tip/PBS/dense FN coverage	0.24 ± 0.06	19.0 ± 1.2
glass/Au tip/water/dense FN coverage	0.25 ± 0.05	20.1 ± 1.1
glass/Au tip/PBS/dense FN coverage	0.20 ± 0.03	18.0 ± 0.57
glass/Si ₃ N ₄ /PBS/dense FN coverage	0.28 ± 0.06	18.9 ± 0.87
mica/Au tip/water/isolated single molecules	0.21 ± 0.095	16.2 ± 1.0
only single rupture plots	$0.020 \pm 1.2 \times 10^{-3}$	14.6 ± 0.18

375 internal friction of the protein need to be investigated
376 further.^{60–66}

377 Conclusions

378 The mechanical behavior of FN molecules that are
379 elongated between an AFM tip and a negatively charged
380 substrate were measured and analyzed. Several solvents,
381 substrates, and tip materials were tested. Plots of
382 distributions of rupture force and the lengths between
383 successive ruptures were measured. Type III domain
384 unfolding events were not predominant when pulling
385 single, isolated molecules on mica. Apparently, the
386 proteins, where isolated from each other, became unstable
387 and underwent partial denaturation at the surface prior
388 to their extension. This would explain the absence of a
389 strong peak at ~ 25 nm, the length observed for mechani-
390 cally unfolding a Type III domain. When the protein's
391 concentration on the surface was increased to the point

of surface aggregation, Type III domain denaturation was
observed to occur in our extension measurements. This
implies that the proteins exposed on the surface did not
undergo surface denaturation before elongating with an
AFM tip. This finding that protein density enhances
protein stability agrees well with other groups' work in
unrelated experiments.^{4–5,13,49} For example, using circular
dichroism, Norde and Favier⁴ measured the structural
rearrangements of bovine serum albumin and hen's egg
lysozyme on silica particles. For both proteins, they
observed a decrease in the α -helix content upon adsorption,
implying surface denaturation, but this effect diminished
upon increasing the protein's surface coverage. Further-
more, in the study by Grinnell and Feld,¹³ they observed
the adsorption characteristics of plasma FN on nonwet-
table bacteriological dishes. They concluded that, at a low
surface concentration, FN was unfolded into an inactive
conformation, but at a higher surface concentration, the
molecular packing requirements prevented unfolding.
Therefore, our results from an AFM prove to be consistent
with other groups' work; however, our technique allows
us to observe the behavior of a single molecule and can
provide additional information such as the details of the
unfolding thermodynamics. Our results could also provide
insight that might be important for designing biocom-
patible substrates suitable for cellular seeding. As recently
reviewed by Mrksich⁶⁷ and reported in a research article
by Garcia et al.,⁶⁸ it was found that different surfaces

(60) Sukhishvili, S. A.; Chen, Y.; Mueller, J. D.; Gratton, E.; Schweizer, K. S.; Granick, S. *Nature* **2000**, *404*, 146.

(61) Jacob, M.; Schmid, F. X. *Biochemistry* **1999**, *38*, 13773.

(62) Swegat, W.; Schlitter, J.; Kruger, P.; Wollmer, A. *Biophys. J.* **2003**, *84*, 1493.

(63) Portman, J. J.; Takada, S.; Wolynes, P. G. *J. Chem. Phys.* **2001**, *114*, 5082.

(64) Plaxco, K. W.; Baker, D. *Proc. Natl. Acad. Sci. U.S.A.* **1998**, *95*, 13591.

(65) Alm, E.; Morozov, A. V.; Kortemme, T.; Baker, D. *J. Mol. Biol.* **2002**, *322*, 463.

(66) Ghatak, A.; Vorvolakos, K.; She, H.; Malotky, D.; Chaudhury, M. K. *J. Phys. Chem. B* **2000**, *104*, 4018.

(67) Mrksich, M. *Chem. Soc. Rev.* **2000**, *29*, 267.

392
393
394
395
396
397
398
399
400
401
402
403
404
405
406
407
408
409
410
411
412
413
414
415
416
417
418
419

420 induce protein conformations that elicit a variety of
421 responses to antibody binding and cellular growth. For
422 example, the binding of HFN7.1, an antibody, to FN on
423 uncharged polystyrene has a FN surface concentration
424 dependence that indicates that protein–protein interac-
425 tions initially enhance antibody binding.⁶⁸ The relation
426 between the concentration dependence we found and its
427 influence on cellular response deserves further investiga-
428 tion.

429 We also found that the most probable force transition
430 events occurring in our single-molecule studies result from
431 a protein–surface interaction. In the aggregate studies,
432 the microruptures for domain unfolding events produced
433 only one linear region in a loading-rate plot, whereas the
434 single-molecule studies produced two. Loading-rate plots
435 of force plots containing only a single rupture, which most
436 likely probe a specific surface–protein interaction, gave

437 rise to two linear regions with parameters very similar to
438 the single-molecule studies. Combining the results of ΔL ,
439 the rupture force, the loading-rate plots, and the ther-
440 modynamic parameters obtained from this analysis, it is
441 concluded that, when pulling single, isolated molecules of
442 FN on mica, domain denaturation is not observed.
443 Apparently, the protein is already partially denatured.

Acknowledgment. We gratefully acknowledge finan- 444
cial support from NSF (PHYS-0103048 and CHE-9816820) 445
and ONR (N00014-02-1-0327). P.Y.M would like to thank 446
A. Tivanski and B. Akhremitchev for their enlightening 447
discussions, her family for their support, and Asylum 448
Research for their generous help. 449

Supporting Information Available: Summary of the 450
rupture forces and differences in length between successive 451
ruptures for the isolated, single-molecule studies and aggregate 452
studies. 453

LA035217W

454

(68) Garcia, A. J.; Vega, M. D.; Boettiger, D. *Mol. Biol. Cell* **1999**, *10*, 785.